JPEDAV (2006) 27:14-21
DOI: 10.1361/105497106X92745
1547-7037/$19.00 ©ASM International

Revolutionary Microstructure Control with Phase Diagram Evaluation for the Design of $E2_1$ Co_3AlC-Based Heat-Resistant Alloys

Yoshisato Kimura, Kiichi Sakai, and Yoshinao Mishima

(Submitted January 7, 2005; in revised form November 4, 2005)

$E2_1$ Co_3AlC might be used as a strengthener to develop new Co-based heat-resistant alloys. To establish the basis of microstructure control for further improving mechanical properties, phase equilibria in the CoAl-C ternary system were investigated and phase diagram information particularly related to $E2_1$ Co_3AlC and liquid phase were evaluated and reconsidered. Single crystals of $E2_1$ Co_3AlC have been grown successfully for the first time using optical floating zone (OFZ) melting. Extra ordering of carbon atoms taking place in $E2_1$ Co_3AlC was confirmed using single crystals by transmission electron microscopy. As a result of this ordering, $E2_1'$ $Co_3AlC_{0.5}$ accompanies formation of antiphase boundaries. A wide variety of the two-phase $Co_3AlC/\alpha(Co)$ microstructures were prepared by unidirectional solidification using OFZ.

Keywords Co_3AlC, microstructure control, optical floating zone melting, phase equilibria

1. Introduction

The $E2_1$-type Co_3AlC is one of a group of exotic intermetallic compounds. It may very likely see use as a strengthener in Co-based heat-resistant alloys because its ordered crystal structure is very similar to that of $L1_2$ Ni_3Al. It is also well known as a perovskite-type structure. The only difference between $E2_1$ and $L1_2$ is distinguished by a carbon atom occupying the octahedral interstice at the body center (Fig. 1a). Because "$L1_2$ Co_3Al" does not exist as a stable phase in the CoAl binary system, addition of carbon to form a CoAl-C alloy could be advantageous in designing Co-based superalloys. Thus $E2_1$ Co_3AlC can be used as an interstitially stabilized "$L1_2$ Co_3Al" phase.

The phase stability of $E2_1$ phases has been extensively investigated for many alloy systems by Huetter et al.,[1,2] Stadelmaier et al.,[3] and Nowotny et al.[4] in the late 1950s through the 1960s, but mechanical properties of $E2_1$ Co_3AlC alloys were not investigated until Hosoda et al.[5] first examined the compressive mechanical behavior of multiphase alloys in 1992. Kimura et al. have been conducting systematic investigations to design and to develop $E2_1$ Co_3AlC-based heat-resistant alloys.[6-14] These investigations, since 1992, consisted of a series of studies on the determination of phase diagrams, microstructure control, evaluation of mechanical properties, and measurements of magnetic properties, all for CoAl-C alloys with and without quaternary additions of Ni or Fe. Recently, Ohtani et al.[15] determined the thermodynamic aspects of the CoAl-C ternary system and its phase diagram by combining ab-initio energetic calculations with a CALPHAD approach. Interest in $E2_1$ Co_3AlC continues to expand.

It was previously reported that the $Co_3AlC/\alpha(Co)$/B2-CoAl three-phase alloys have a good balance between elevated temperature strength and ambient temperature ductility: yield strength of exceeding 350 MPa at 1273 K[6,8] and beyond 8% plastic deformability in tension at room temperature.[9] These desirable values of strength and ductility occur despite the inhomogeneous microstructures in which dendrite morphology of the as-cast state remains present after annealing. Thus, we believe that mechanical properties can be further improved by microstructure control to fabricate homogeneous $Co_3AlC/\alpha(Co)$ two-phase microstructures with the Co_3AlC phase uniformly distributed in ductile $\alpha(Co)$ phase. Another interesting feature of $E2_1$ Co_3AlC is the extra ordering of carbon atoms. This was first observed by Wei et al.[11] to occur in multiphase alloys coexisting with $\alpha(Co)$ solid solution, B2-CoAl, or graphite phases. $E2_1'$ $Co_3AlC_{0.5}$ is formed as a result of this ordering, the ordered structure of which is shown in Fig. 1(b). Recently, it was proposed that this ordering of carbon is most likely due to minimizing the free energy via elastic and magnetic contributions.[13,14]

Phase diagrams play a very important role in alloy design: not only can phase equilibria be known but possible microstructures can also be forecast that could be controlled by a combination of alloying and heat treatment. A good example illustrating how phase diagrams are used in practice is the present investigation of the design and development of $E2_1$ Co_3AlC-based heat-resistant alloys. In the present work, microstructure control has been conducted using optical floating zone (OFZ) melting, which includes

This paper was presented at the International Symposium on User Aspects of Phase Diagrams, Materials Solutions Conference and Exposition, Columbus, Ohio, 18-20 October, 2004.

Yoshisato Kimura, Kiichi Sakai, and **Yoshinao Mishima,** Tokyo Institute of Technology, Materials Science and Engineering, 4259-G3-23, Nagatsuta Midori-ku, Yokohama 226-8502, Japan. Contact e-mail: kimurays@materia.titech.ac.jp.

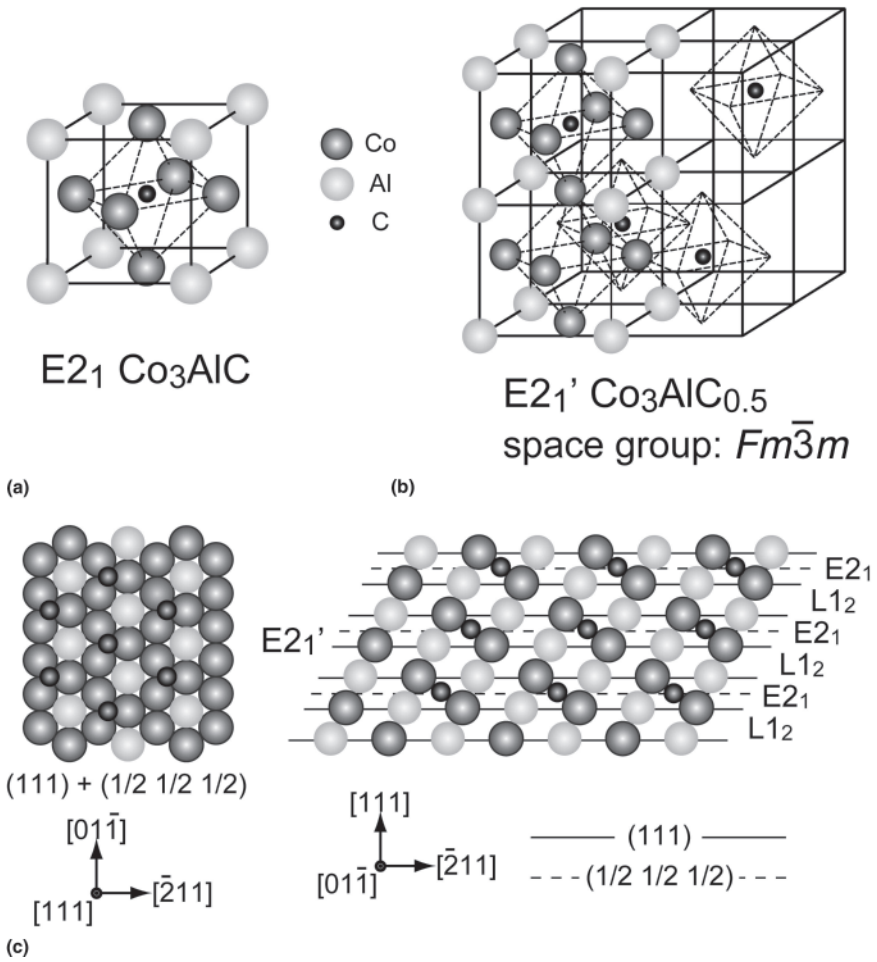

Fig. 1 Unit cells of E2$_1$ Co_3AlC and E2$_1$′ $Co_3AlC_{0.5}$

growing single crystals and controlling lamellar microstructures. The objective of the present work is to establish the basis for the microstructure control on E2$_1$ Co_3AlC-based alloys to achieve much better performance of both high-temperature strength and ambient-temperature ductility. Ideal microstructures must have a homogeneous distribution of $Co_3AlC/\alpha(Co)$ (two-phase). It is necessary to evaluate or to reconsider several pieces of information concerning the CoAl-C ternary-phase diagram, particularly the phase equilibria involving Co_3AlC and the liquid phase. Moreover, the extra ordering of carbon atoms and the formation of E2$_1$′ $Co_3AlC_{0.5}$ were investigated in more detail using single crystals.

2. Experimental Procedures

Several Co_3AlC-based multiphase alloys were prepared by arc melting in an Ar gas atmosphere. To ensure high carbon contents for Co_3AlC alloys, master alloy ingots were preliminarily made by induction heat melting. Unidirectional solidification was conducted using OFZ melting to grow Co_3AlC single crystals and $Co_3AlC/\alpha(Co)$ two-phase alloys. Sample preparations were made in the OFZ furnace equipped with four xenon lamps under an Ar gas flow after evacuation. Microstructures were observed and characterized by means of scanning electron microscopy (SEM-BEI) and transmission electron microscopy (TEM). Phase identification and crystal structure analysis were performed using x-ray diffractometry (XRD) and selected area diffraction (SAD) pattern analysis of TEM. Chemical compositions were quantitatively measured for each constituent phase using electron probe microanalysis (EPMA) with a wavelength dispersive x-ray spectrometer (WDS) (Jeol JXA-8900). The carbon concentration was measured with special care using LDE2 as a crystal for the spectrometer of EPMA. Pure graphite was used as the standard reference. Measurements were conducted with an accelerating voltage of 15 kV using a cold trap. The surfaces of specimens were mirror-finished, and masking with a Cu-film was used to provide a conducting conduit to drain any induced surface charge. Rather than using the so-called ZAF correction, a slight adjustment was performed by comparing the energy profiles between the specimens and the reference materials, such as carbides. Such an adjustment is very small because the carbon concentration in the E2$_1$ (E2$_1$′) phase is sufficiently high enough for accurate measurements, being higher than 1 wt.%. Antiphase domain (APD) size was con-

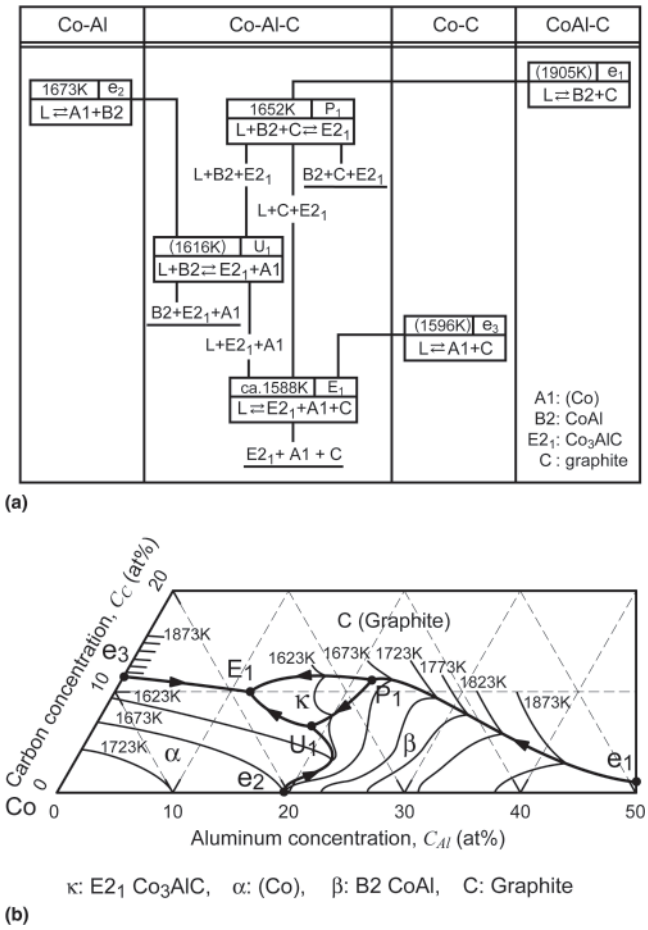

Fig. 2 (a) Reaction scheme and (b) projection of the liquidus surface of the Co-Al-C phase diagram evaluated for the Co-rich corner

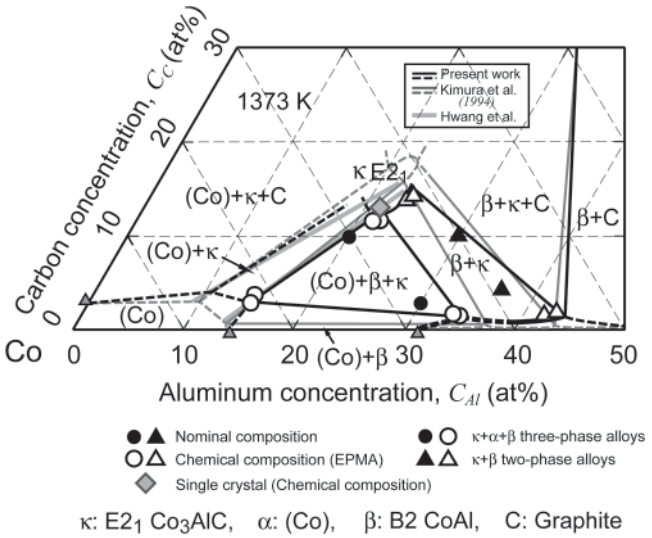

Fig. 3 Isotherm of the Co-Al-C phase diagram evaluated at 1373 K for the Co-rich corner

trolled by the heat treatment; annealing at 1373 K for 24 h or at 1073 K for 24 h, followed by water quenching differential scanning calorimetry (DSC) was used to measure the $E2_1'$, ordering temperature of carbon, T_o^{chem}, and the Curie temperature, T_C^{mag}, in a temperature range from 300 to 1273 K at heating and cooling rates of 10 K/min.

3. Results and Discussion

3.1 Phase Equilibria in the CoAl-C Ternary System

Pieces of phase diagram information were reconfirmed and revised because phase equilibria regarding solidification sequence are quite important in considering microstructure control. The most updated versions of the CoAl-C ternary-phase diagram are represented in Fig. 2 and 3. Our previous evaluation[7] had been conducted on the basis of the phase diagram reported by Huetter et al.[2,16] The reaction scheme of CoAl-C ternary system and the projection of corresponding liquidus surface are represented in Fig. 2(a) and (b). Very slight revisions were made for the chemical compositions of the invariant reactions, P_1 and U_1, judging by the microstructures of several arc-cast alloys and considering the microstructures of OFZ alloys. $E2_1$ Co_3AlC forms by the ternary peritectic reaction, P_1, previously evaluated at 1652 K. The isotherm at 1373 K (Fig. 3) was revised mainly for the $Co_3AlC/\alpha(Co)/CoAl$ three-phase field and its related phase boundaries using EPMA. Nominal compositions of four alloys measured by EPMA are indicated (solid symbols in Fig. 3) together with the chemical composition of each constituent phase (open symbols).

The chemical composition of a single crystal has been evaluated as 66.7 at.% Co-20.6 at.% Al-12.7 at.% C. It is slightly Co-rich and Al-lean composition from the ratio of Co/Al = 3:1. This result is rationally accepted because excess Co atoms occupy the Al site while the opposite site occupancy seems not to be allowed. The carbon content is much less than the stoichiometry of ordinary $E2_1$ Co_3AlC but is slightly higher than the stoichiometry of extraordered $E2_1'$. It is known that most $E2_1$ T_3MC, where T is a transition metal and M is a non-transition metal, and the carbon content usually less than the stoichiometric composition,[1-4] and therefore it should be denoted in a strict notation as Co_3AlC_x, where x is about 0.6 in the present case. To the authors' best knowledge, the extra ordering of carbon is observed only in Co_3AlC and Ti_3AlC.[11,17] Note that the ordering of carbon in Ti_3AlC differs from the present $E2_1'$ structure.[17]

3.2 Growth of Single-Crystal Co_3AlC

Single crystals or even single-phase poly-crystals of Co_3AlC have never been produced. As shown in Fig. 2(b), there exists a region in which Co_3AlC is the primary phase that solidifies to the same extent as its compositional range. Nevertheless, it was very hard to prepare the Co_3AlC single-phase alloy, mostly because Co_3AlC is formed by a peritectic reaction involving graphite. It is further complicated by the fact that the single-phase region of Co_3AlC is situ-

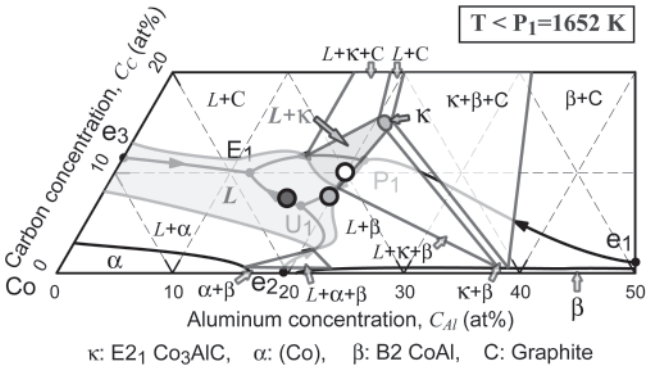

Fig. 4 Schematic isotherm of the Co-Al-C phase diagram estimated at temperature $T < P_1$

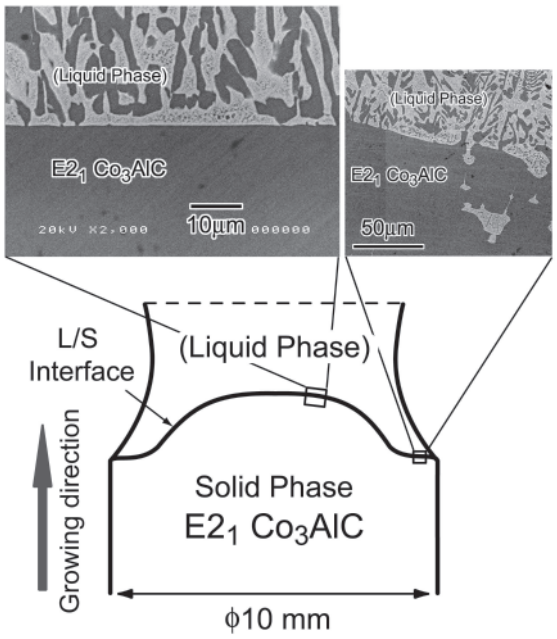

Fig. 5 Back-scattered electron images showing the liquid-solid interface after quenching together with a schematic of longitudinal section of OFZ-grown ingot

ated at a higher carbon concentration than its primary solidification region. The authors have succeeded in growing Co_3AlC single crystals for the first time ever using the OFZ technique with a traveling solvent effect. An isotherm of the CoAl-C phase diagram estimated below the P_1 temperature, $T < P_1$, is drawn in Fig. 4. The authors have selected the nominal composition of seed and feed rods used for OFZ as 70Co-20Al-10C. Carbon content is allowed in a range about 10-12 at.% balancing with cobalt content, and the aluminum content is fixed at 20 at.%. A single crystal grows in a two-phase equilibrium between Co_3AlC and liquid as indicated in the figure. The OFZ conditions for single-crystal growth under flowing Ar gas atmosphere are growth rate, 2.0 mm h^{-1}; rotational speed, 25 rpm.

To observe the liquid-solid interface, the microstructure was frozen during the stable growth by cutting off the lamp power during OFZ. A longitudinal section is shown in Fig. 5 together with a schematic. Carbon atoms are fully consumed as the single crystal grows, and excess cobalt atoms are ejected to enrich the liquid phase. Thus, the resultant single-crystal ingot is surrounded by relatively thin outer layer of Co-rich material. In addition, small α(Co) dendrites are locally observed in the immediate vicinity of the outer layer, on the shoulder of the interface seen in the longitudinal section.

3.3 Ordering of Carbon Atoms in $E2_1$ Co_3AlC and Formation of $E2_1'$ $Co_3AlC_{0.5}$

The extra ordering of carbon atoms was confirmed to occur in the $E2_1$ Co_3AlC single crystal by TEM observation. This ordering of carbon atoms in $E2_1'$ $Co_3AlC_{0.5}$ is accompanied by the formation of antiphase boundaries (APB) with two crystallographic variants. The unit cell of $Co_3AlC_{0.5}$ and its atomic arrangement and stacking sequence of (111) planes are represented in Fig. 1(b) and (c). The $E2_1'$ structure is composed of $L1_2$ and $E2_1$ stacking; hence $E2_1'$ sometimes behaves more like $L1_2$ than $E2_1$, exhibiting excellent plastic deformability and ferromagnetism.[13,14] Figure 6 represents dark-field images (DF) and the corresponding selected area diffraction (SAD) pattern taken from the single crystal with the incident beam direction IB = [011], where (a) and (b) are as-grown and (c) and (d) are water quenched from 1373 K after 24 h of annealing. Sets of <½ ½ ½> diffraction spots observed in SAD pattern indicate the ordered structure of $E2_1'$ $Co_3AlC_{0.5}$. Contrast of APB is only visible in [½ −½ ½]DF (Fig. 6a,c) but is invisible in [100]DF (Fig. 6b,d). This means that this APB has originated from the ordering of carbon atoms being related to the $E2_1'$ structure. The lattice parameter of Co_3AlC, i.e., a half of a lattice parameter of $Co_3AlC_{0.5}$, is measured as 0.36 nm by XRD.

The chemical ordering temperature of carbon atoms, T_o^{chem}, has been estimated at about 1325 K by DSC measurements. We can also confirm T_C^{chem} by the antiphase domain (APD) size, which changes depending on annealing conditions, although the size measurement is not very precise. Relatively coarse APDs are observed in the as-grown state (Fig. 6a), and they are coarsened by annealing at relatively high temperatures below T_C^{chem}. On the other hand, APD size is very fine, of the order after water quenching from 1373 K above T_C^{chem} of several nanometers (Fig. 6c). This suggests that the formation of APB is not fully suppressed by water quenching. Moreover, the authors have reported that $E2_1'$ $Co_3AlC_{0.5}$ exhibits ferromagnetism, and the Curie temperature, T_C^{mag}, determined using a single crystal is around 1115 K. Vibrating sample magnetometry and DSC were used for T_C^{mag} measurements.[13,14] Results indicate that chemical and magnetic ordering must be correlated with each other.

3.4 Various Co_3AlC/α(Co) Two-Phase Microstructures Grown by OFZ

Three nominal alloy compositions (in at.%) were selected for directional solidification of two-phase Co_3AlC/

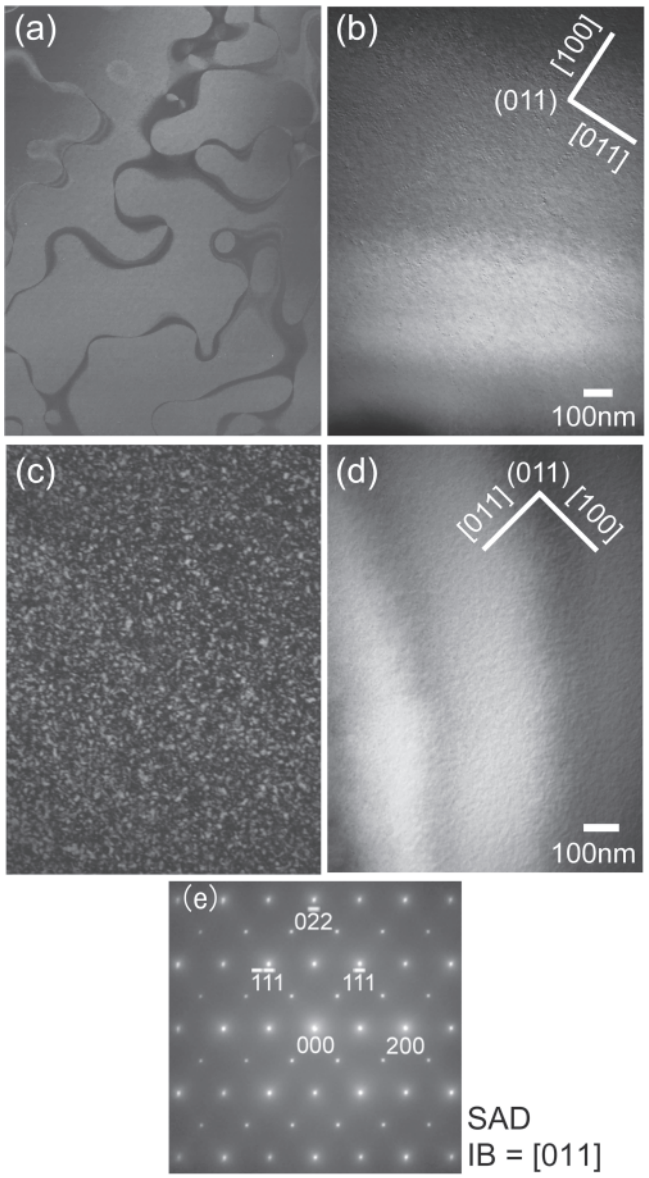

Fig. 6 (a-d) Dark-field images and (e) corresponding selected area diffraction pattern taken from a single crystal: (a,b) as-grown and (c,d) water-quenched from 1373 K after 24 h of annealing; (a,c) [½ −½ ½] DFI and (b,d) [100] DFI

α(Co) microstructure; 70Co-20Al-10C, 72Co-20Al-8C, and 76Co-16Al-8C. Those compositions are indicated on a schematic isotherm in Fig. 4.

The $Co_3AlC/\alpha(Co)$ two-phase lamellar microstructure has been nicely aligned parallel to the growth direction using OFZ with nominal composition of 76Co-16Al-8C as represented in Fig. 7(a) transverse section and (b) longitudinal section parallel to the direction of growth. This lamellar structure is not formed by the eutectic reaction in a strict sense because freedom is not zero with respect to the phase rule. Temperature is a variable regarding three phase equilibrium, liquid, Co_3AlC and α(Co), in the ternary system. Finally, the solidified product consisting of two-phase $Co_3AlC/\alpha(Co)$ is scarcely seen in the continuous α(Co) matrix. One disadvantage of using OFZ in the CoAl-C system would be that the reproducibility is not very good because the growth conditions and very sensitive to small changes in solidification conditions. Paradoxically, it is possible to control microstructure by modifying the growth conditions. The most important factors to control solidification, and therefore the resultant microstructures are temperature gradient, diffusivity, and partitioning of elements across the liquid-solid interface.[18,19] Formation of either a planar-type interface or a cellular-type interface depends on these factors, and the morphology of microstructures is governed by these conditions of liquid-solid interface during solidification. Nevertheless, what we can control are the OFZ conditions: solidification rate, rotational speed, and lamp power (i.e., temperature).

An isotherm estimated below the U_1 temperature, $T < U_1$, and an isopleth along the compositional line including 70Co-20Al-10C and 76Co-16Al-8C are schematically drawn in Fig. 8(a) and (b), respectively. Regions involving liquid and Co_3AlC phases, liquid/Co_3AlC and liquid/$Co_3AlC/\alpha(Co)$, are situated in a wide compositional range but also in narrow temperature range of about 50 K, as indicated by the schematic isopleth. It suggests that a slight change in temperature leads to a drastic change in equilibrium composition of each constituent phase. Moreover, the three-phase equilibrium of liquid/$Co_3AlC/\alpha(Co)$ at the liquid/solid interface may easily vary with a small change in temperature because the liquid/$Co_3AlC/\alpha(Co)$ three-phase triangle in an isotherm is compositionally quite narrow. These aspects can be a cause of unstable growth in the present case of $Co_3AlC/\alpha(Co)$ two-phase alloys.

Figure 7 shows a variety of $Co_3AlC/\alpha(Co)$ two-phase microstructures grown by OFZ. Even at the same nominal composition, the morphology of the microstructure varies widely depending on the OFZ conditions or their fluctuation. Factors that can be intentionally controlled are, basically, the growth rate and the rotational speed; however, it is very hard to theoretically describe the formation of microstructures by these factors, as discussed above. In the case of 76Co-16Al-8C, increasing the volume fraction of Co_3AlC phase yields a lamellar microstructure with coarse primary Co_3AlC dendrites, as shown in Fig. 7(c) transverse and (d) longitudinal sections, yet the alloy has a rather homogeneous microstructure at this length scale. The most interesting case would be 70Co-20Al-10C, which is selected for single-crystal growth. If temperature and/or chemical composition shift slightly from ideal conditions, any increment in the volume fraction of α(Co) leads to formation of cellular-type microstructures, as shown in Fig. 7(e) through (g). Due to the enriched Co content in the liquid near the interface, the solidification temperature would be lower than the case of single-crystal growth, and the rotational speed would be insufficient to avoid the compositional supercooling. These cellular-type microstructures may not be very stable. Nevertheless, they are thought to be adequate microstructures for both ambient temperature ductility and high-temperature strength because they have the homogeneous two-phase microstructure con-

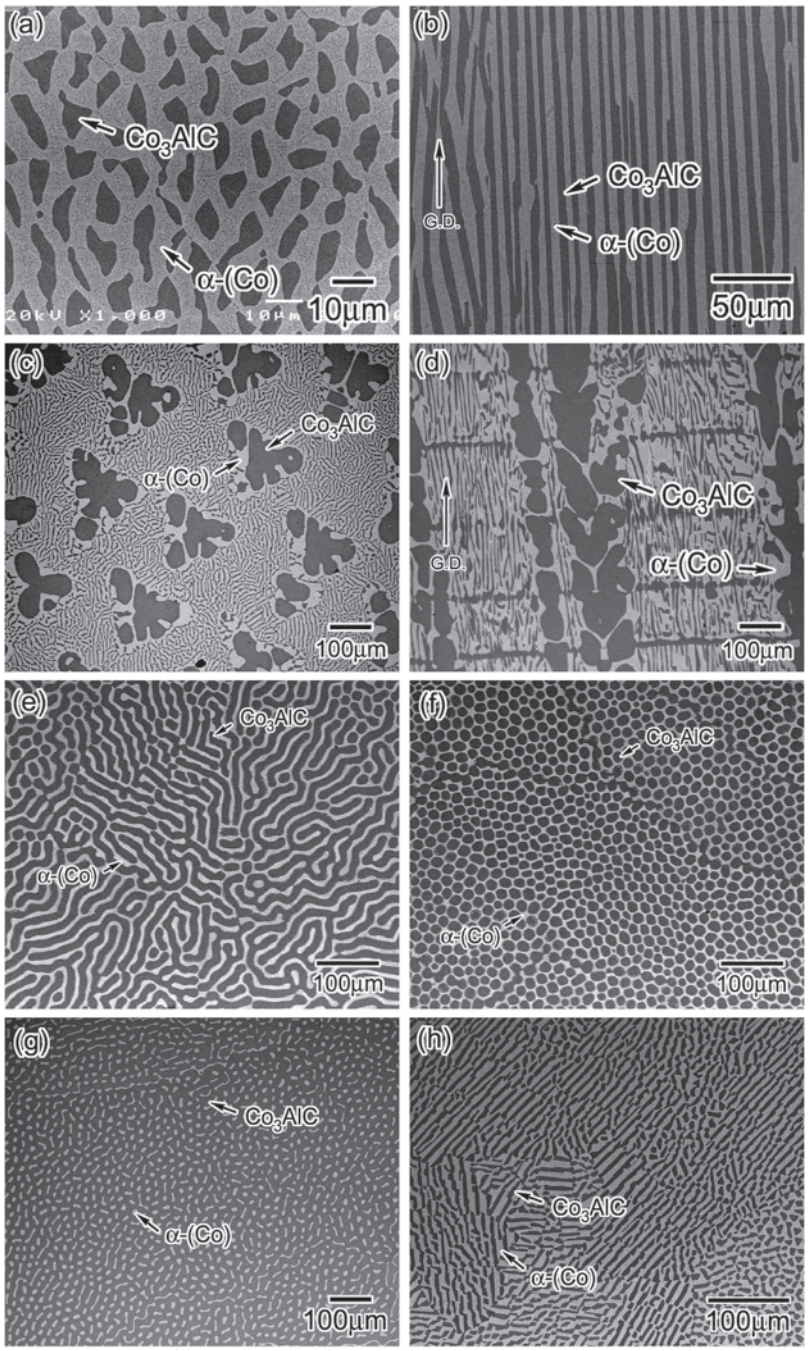

Fig. 7 Wide variety of $Co_3AlC/\alpha(Co)$ two-phase microstructures prepared by unidirectional solidification using OFZ, with the following growth rates (GR, mm h^{-1}) and rotational speeds (RS, rpm): (a,b) GR = 10, RS = 26; (c,d) GR = 10, RS = 45; (e) GR = 2, RS = 25; (f) GR = 2, RS = 25; (g) GR = 2, RS = 45; and (h) GR = 2, RS = 45. Alloys used: (a-d) 76Co-16Al-8C, (e-g) 70-20Al-10C, and (h) 72Co-20Al-8C, with (a,c,e-h) transverse section and (b,d) longitudinal section shown

sisting of Co_3AlC and α(Co). Continuous networks of α(Co) are formed in the Co_3AlC matrix (Fig. 7e,f), or fine particles of α(Co) are distributed in the Co_3AlC matrix (Fig. 7g). Microstructures shown in Fig. 7(e) and (f) are grown under the same nominal conditions, although local changes such as the condition of the interface and the volume fractions of two phases could cause a different morphology of the microstructures that are formed. Fully lamellar microstructure with homogeneous morphology can be fabricated at 72Co-20Al-8C, as represented in Fig. 7(h). Further trial and error is required to precisely optimize the OFZ conditions for stably growth of homogeneous microstructures. However, the present results provide hope for accomplishing revolutionary microstructure control of $Co_3AlC/\alpha(Co)$ two-phase heat-resistant structural alloys using OFZ.

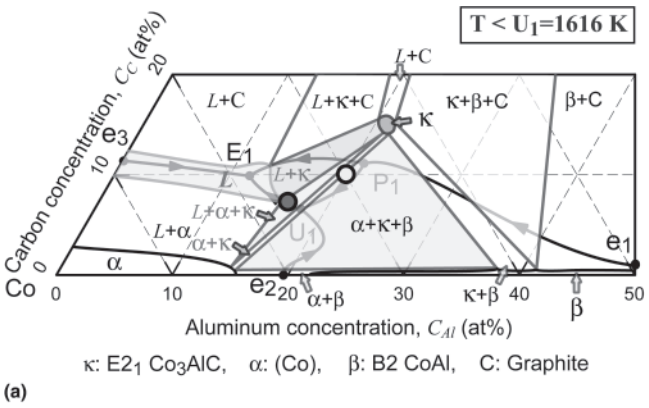

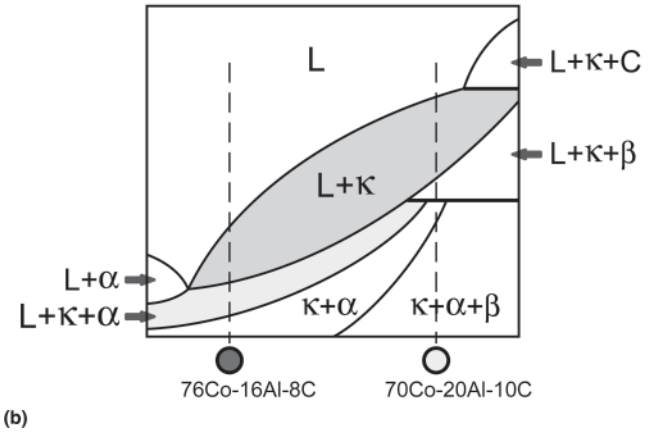

Fig. 8 Schematic drawing of Co-Al-C phase diagrams: (a) isotherm estimated at temperature, $T < U_1$, and (b) isopleth along the compositional line including 70Co-20Al-10C and 76Co-16Al-8C

4. Conclusions

The CoAl-C phase diagram has been evaluated and considered, particularly for phase equilibria involving Co_3AlC and liquid phase for the purpose of furthering our alloy design of Co_3AlC-based heat-resistant structural alloys. Microstructure control, including single-crystal growth and eutectic lamellar microstructures, was performed using OFZ melting. The following concluding remarks are drawn from the present work.

- Some pieces of phase diagram information of Co-Al-C ternary system were reconsidered and evaluated experimentally; the results generated a projection of liquidus surface, an isotherm at 1373 K, and schematic isotherms and isopleths at $T < P_1$ (temperature less than the temperature of the ternary peritectic invariant).
- Single crystals of $E2_1$ Co_3AlC have been successfully grown for the first time using OFZ. The extra ordering of carbon atoms and the formation of $E2_1'$ Co_3AlC with antiphase boundaries were confirmed in single crystals by TEM observation.
- A variety of Co_3AlC/α(Co) two-phase microstructures were prepared by unidirectional solidification using OFZ. Homogeneous distribution of Co_3AlC/α(Co) two-phase alloys having different morphology could be controlled by OFZ, which indicates the possibility of microstructure control for further improving mechanical properties in high-temperature structural applications.

Acknowledgments

The present work was extended and conducted on the ground work previously supported by the PRESTO program, Organization and Function, Japan Science and Technology Agency. The authors are grateful to Assoc. Prof. Hiroshi Ohtani, Kyushu Institute of Technology, Assoc. Prof. Hideki Hosoda, Tokyo Institute of Technology, and Dr. Fu-Gao Wei, National Institute for Materials Science for their helpful comments and discussions.

References

1. L.J. Huetter and H.H. Stadelmaier, Ternary Carbides of Transition Metals with Aluminum and Magnesium, *Acta Metall.,* 1958, 6, p 367-370
2. L.J. Huetter, H.H. Stadelmaier, and A.C. Fraker, Über das Ternäre System Kobalt-Aluminium-Kohlenstoff, *Metallwiss. Technol.,* 1960, 14, p 113-115, in German
3. H.H. Stadelmaier, Metal-Rich Metal-Metalloid Phases, *Developments in the Structural Chemistry of Alloy Phases,* B.C. Giessen, Ed., Plenum Press, New York, 1969, p 141-180
4. H. Nowotny and F. Benesovsky, Phase Stability and Crystal Chemistry of Complex Compounds Containing Transition Elements and Nonmetals, *Phase Stability in Metals and Alloys,* R.S. Rudman, Ed., McGraw Hill, New York, 1967, p 319-336
5. H. Hosoda, M. Takahashi, T. Suzuki, and Y. Mishima, Mechanical Properties of Co Alloys Based on $E2_1$ Type Co_3AlC Intermetallic Compound, *High-Temperature Ordered Intermetallic Alloys V,* Volume 288, *MRS Symp. Proc.,* Materials Research Society, 1993, p 793-798
6. Y. Kimura, M. Takahashi, S. Miura, and Y. Mishima, Phase Stabilities and Mechanical Properties of Multi-Phase Alloys Based on the B2 CoAl and the $E2_1$ Co_3AlC, *High-Temperature Ordered Intermetallic Alloys VI,* Volume 364, *MRS Symp. Proc.,* Materials Research Society, 1995, 1371-1376
7. Y. Kimura, M. Takahashi, S. Miura, T. Suzuki, and Y. Mishima, Phase Stabilities and Relations of Multi-Phase Alloys Based on B2 CoAl and $E2_1$ Co_3AlC, *Intermetallics,* 1995, 3, p 413-425
8. Y. Kimura, M. Takahashi, H. Hosoda, S. Miura, and Y. Mishima, Compressive Mechanical Properties of Multi-Phase Alloys Based on B2 CoAl and $E2_1$ Co_3AlC, *Intermetallics,* 2000, 8, p 749-757
9. Y. Kimura, C.T. Liu, and Y. Mishima, Microstructure Control and Tensile Properties of the Three-Phase Alloys Based on the $E2_1$ Co_3AlC and B2 CoAl, *Intermetallics,* 2001, 9, p 1069-1078
10. K.-Y. Hwang, Y. Kimura, S. Miura. and Y. Mishima, Mechanical Properties of Co-Base Alloys Strengthened by $E2_1$-Type Intermetallic Compound Co_3AlC, *Proc. 3rd Pacific Rim Int. Conf. Mater., PRICM-3,* TMS, 1998, p 2355-2360
11. F.-G. Wei, K.-Y. Hwang, and Y. Mishima, Deformation of $Co_3AlC_{0.5}$ and a $Co_3AlC_{0.5}$-Strengthened Cobalt-Based Alloy, *Intermetallics,* 2001, 9, p 671-679
12. Y. Kimura, K. Iida, and Y. Mishima, Phase Stability and Magnetic Properties of $E2_1$-$(Co,Ni)_3AlC$ Based Alloys, *Defect Properties and Related Phenomena in Intermetallic Al-*

loys, Volume 753, *MRS Symp. Proc.,* Materials Research Society, 2003, p 433-438

13. Y. Kimura, K. Sakai, F.-G. Wei, and Y. Mishima, "Phase Stability, Ordered Structures and Magnetic Properties of $E2_1$-Based Co_3AlC_x," Intl. Symp. Nano-org. Funct., Japan Science and Technology Agency, Tokyo, 2004
14. Y. Kimura, F.-G. Wei, H. Ohtsuka, and Y. Mishima, Magnetic Properties of $E2_1$-Base Co_3AlC and the Correlation with the Ordering of Carbon Atoms and Vacancies, *Integrative and Interdisciplinary Aspects of Intermetallics,* Volume 842, *MRS Symp. Proc.,* Materials Research Society, 2005, p 395-400
15. H. Ohtani, M. Yamano, and M. Hasebe, Thermodynamic Analysis of the Co-Al-C and Ni-Al-C Systems by Incorporating ab Initio Energetic Calculations into the CALPHAD Approach, *CALPHAD,* 2004, 28, p 177-190
16. B. Grieb and H.H. Stadelmaier, *Ternary Alloys,* Volume 4, G. Petzow and G. Effenberg, Eds., VCH, Weinheim, 1991, p 465-468
17. W.-H. Tian, T. Sano, and M. Nemoto, Structure of Perovskite Carbide and Nitride Precipitates in $L1_0$-Ordered TiAl, *Phil. Mag. A,* 1993, 68, p 965-976
18. H. Bei, E.P. George, E.A. Kenik, and G.M. Pharr, Directional Solidification and Microstructures of Near-Eutectic Cr-Cr_3Si Alloys, *Acta Mater.,* 2003, 51, p 6241-6252
19. M.C. Flemings, *Solidification Processing*, *Materials Science and Engineering Series,* McGraw-Hill, New York, 1974, p 31-133